TÜBİTAK

Turkish Journal of Physics

http://journals.tubitak.gov.tr/physics/

Research Article

Turk J Phys
(2018) 42: 649 – 658
© TÜBİTAK
doi:10.3906/fiz-1806-15

One-dimensional fluid and hybrid numerical analysis of the plasma properties in the discharge channel of a Hall thruster

Çinar YÜNCÜLER[1], **İsmail RAFATOV**[2,*], **Demet ULUŞEN**[1]
[1]TÜBİTAK Space Technologies Research Institute, Ankara, Turkey
[2]Department of Physics, Faculty of Arts and Sciences, Middle East Technical University, Ankara, Turkey

Received: 13.06.2018 • **Accepted/Published Online:** 18.09.2018 • **Final Version:** 14.12.2018

Abstract: One-dimensional fluid and hybrid fluid–kinetic numerical codes are developed and applied to the analysis of axial distributions of plasma properties in the discharge channel of a Hall-effect thruster. Within the hybrid model ions are described by the kinetic Vlasov equation, while electrons and neutral atoms are treated as fluids. The results obtained from fluid and hybrid models are compared. Different operating regimes such as damped, periodic, and aperiodic irregular oscillations about the stationary state are observed and discussed. Thrust and efficiency of the thruster for different input parameters are estimated.

Key words: Hall effect thruster, gas discharge, plasma, numerical simulation

1. Introduction

Hall thrusters are propulsion devices that are used on spacecrafts for maneuvering and orbit control purposes. They provide significantly higher specific impulse in comparison with chemical propulsion systems. Therefore, by using a Hall thruster, the amount of required propellant mass for a space mission can be reduced. This advantage has been the reason for the significant demand for such thrusters over the last 40 years. The first satellite equipped with a Hall thruster, "Meteor", was put into orbit in 1971 and since then more than 200 Hall thrusters have been operating in space [1].

A Hall thruster consists of an annular channel with an interior anode at its base and an external cathode near the channel exit. Propellant gas (usually xenon) is injected into the channel from the anode surface. Electrons supplied by the cathode ionize the propellant through collisions. A magnetic circuit creates a radial magnetic field across the channel, which prevents electrons from moving directly to the anode. The electrons with reduced mobility due to the transverse magnetic field spiral along the field lines, drifting in the $\mathbf{E} \times \mathbf{B}$ direction and creating an azimuthal Hall current. This permits the applied discharge voltage to be distributed along the channel axis in the quasi-neutral plasma. Therefore, an axial electric field is established between the anode at the channel base and the cathode [2, 3]. The ionized propellant is then accelerated by the electric field and reaches very high exhaust velocities ($\sim 16,000$ m/s) at the channel exit, resulting in the generation of thrust.

Numerical models of Hall thrusters have been evolving during the past 20 years. These models give an insight into the physical processes within the discharge channel, predict the performance of thrusters, and

*Correspondence: rafatov@metu.edu.tr

determine parameters such as thrust and specific impulse. In recent years, fluid [4, 5], fully kinetic [6], and hybrid [7–9] methods have been developed for both 1D and 2D analyses of Hall thrusters. In kinetic models, for each plasma species particle motion is described by the velocity distribution function obtained from the solution of the Boltzmann equation. Although kinetic modeling is advantageous in providing detailed information about the physics of plasma processes, it is not practical due to the very long computation time required. Fluid models include continuity, momentum, and energy equations that are derived by taking moments of the Boltzmann equation in velocity space. Therefore, plasma properties of interest in fluid models are macroscopic quantities. Although these models are computationally more efficient, they do not represent all the physical aspects adequately. Hybrid modeling, where electrons are modeled as fluid while neutrals and ions are treated as particles, is a compromise between the approaches mentioned above.

Pioneering contribution to the design and implementation as well as theoretical analysis of Hall-effect thrusters (which are usually called stationary plasma thrusters in the Russian literature) was done by Morozov (see, e.g., [2, 10–12]). Numerical study of axial distributions of plasma properties in the discharge channel of a Hall-effect thruster in [11, 12] revealed the existence of different steady and unsteady operating regimes, which were found to be in reasonably good agreement with experimental results.

In the present work, numerical codes based on fluid and hybrid models are developed for stationary and transient 1D analysis of a Hall-effect thruster. In order to test and verify the validity of the numerical codes, we mainly followed the approach proposed in [10–12]. Details of the models are introduced in Section 2. The results and discussions are presented in Section 3. Finally, Section 4 contains the conclusions.

2. Model

The model is one-dimensional so that plasma variables are uniform in the radial and the azimuthal directions but change in the axial x direction along the discharge channel. The computational domain is bounded by the anode surface at $x = 0$ and the channel exit at $x = L$, where the cathode is placed.

Xenon is used as the propellant. Three species are considered in the model: Xe atoms, Xe^{+} ions, and electrons. Although Xe^{+2} ions may also exist inside the channel, they are neglected in this model. Ions are insensitive to the magnetic field since their Larmor radius is much greater than the channel dimensions [3] and they leave the discharge channel without collisions [9].

Xe atoms are injected into the discharge channel with a given velocity V_a. Since no force is acting on them, they move with this constant velocity along the channel [9]. Therefore, the momentum equation for neutral atoms is eliminated.

The plasma is assumed to be quasi-neutral. Thus, everywhere along the discharge channel, ion and electron number densities are assumed to be equal, $n_i \approx n_e$. As a result, the axial electric field is not obtained from Poisson's equation but is calculated using Ohm's law.

In Hall thrusters, the magnetic field induced by the motion of charged particles is small compared to the externally applied magnetic field. Therefore, the magnetic field is assumed to be static and approximated analytically.

2.1. Fluid approach

We developed the model essentially as in [10, 11]. The governing equations are the ion continuity and momentum equations and the neutral atom continuity equation:

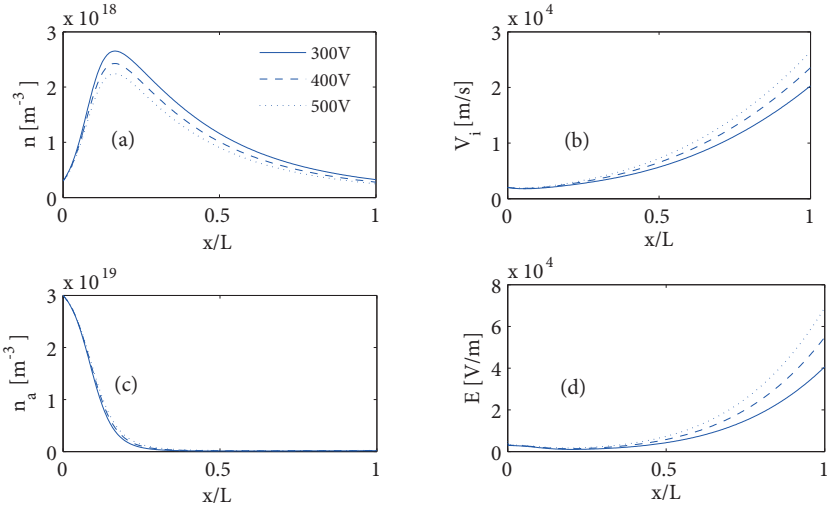

Figure 1. Stationary solutions obtained from the fluid model. Profiles of (a) ion number density, (b) ion velocity, (c) neutral atom number density, and (d) electric field along the discharge channel, obtained under discharge voltages $U_0 =$ 300, 400, and 500 V. Flow rate is $\dot{m} = 3.25$ mg/s.

$$\frac{\partial n}{\partial t} + \frac{\partial nV}{\partial x} = \beta n n_a, \tag{2.1}$$

$$\frac{\partial nV}{\partial t} + \frac{\partial nV^2}{\partial x} = \frac{en}{M}E + \beta n n_a V_a, \tag{2.2}$$

$$\frac{\partial n_a}{\partial t} + V_a \frac{\partial n_a}{\partial x} = -\beta n n_a. \tag{2.3}$$

Here M is the mass of Xe atoms. The source term of the ion continuity equation (Eq. (2.1)) represents the ion generation with rate β. The second term on the right-hand side of Eq. (2.2) represents the momentum contribution by the ionized atoms having a velocity V_a before ionization. As mentioned above, the neutral atom velocity, V_a, is constant throughout the channel. The source term of the continuity equation for neutral Xe atoms represents the neutral atom depletion due to ionization.

The electric field is determined from Ohm's law:

$$E = \frac{1}{\sigma}\left(J - J_i\right), \tag{2.4}$$

where $J_i = enV$, σ is plasma conductivity defined as a function of the magnetic field, $\sigma(x) = \sigma_0 \left[B_0/B(x)\right]^2$, where the profile of the transverse magnetic field is described as $B(x) = B_0\left[b_0 + (1-b_0)(x/L)^2\right]$, where $b_0 = B(0)/B_0$, which is consistent with the actual magnetic field profiles in the stationary plasma thrusters [10, 11].

The set of equations becomes complete with the equation for the electric circuit:

$$L_c \frac{dJ}{dt} + RJ + \int_0^L E dx = U_0, \tag{2.5}$$

where U_0 is the discharge voltage, L_c is the inductance, and R is the resistance.

The boundary conditions are imposed at the anode surface of the computational domain:

$$n(0,t) = n_0,\ n_a(0,t) = n_{a0},\ V(0,t) = V_0. \tag{2.6}$$

2.2. Hybrid method approach

In the hybrid method, ions are treated using the kinetic approach; the ion distribution function $f(x,V,t)$ is thus obtained by solving the 1d1v (one-dimensional in coordinate and velocity spaces) Vlasov equation. Neutral atoms and electrons are treated as fluids. The electron energy equation is also included in the model in order to account for the role of the electron heat conduction.

The hybrid model contains the ion kinetic equation, the continuity equation for the neutral atoms, and the electron energy equation [2, 10, 12]:

$$\frac{\partial f}{\partial t} + V\frac{\partial f}{\partial x} + \frac{eE}{M}\frac{\partial f}{\partial V} = \beta(T) n n_a \delta(V - V_a), \tag{2.7}$$

$$\frac{\partial n_a}{\partial t} + V_a\frac{\partial n_a}{\partial x} = -\beta(T) n n_a, \tag{2.8}$$

$$\frac{3}{2}\left(\frac{\partial nT}{\partial t} + \frac{\partial nV_eT}{\partial x}\right) = -\frac{\partial nV_eT}{\partial x} + \frac{\partial}{\partial x}\left(\kappa_e\frac{\partial T}{\partial x}\right) + J_eE - \alpha\beta(T) n n_a. \tag{2.9}$$

The right-hand side of Eq. (2.7) represents the ion production. δ denotes the Dirac delta function: it is assumed that the newly generated ions are introduced with a velocity equal to the neutral atoms velocity V_a [9].

The system, as well as in the case of a fluid model, is completed with Ohm's law (2.4) and the equation of the electric circuit (2.5).

The macroscopic quantities such as the ion number density n in Eqs. (2.7) and (2.8) and the ion flux J_i in Eq. (2.4) are derived using the ion distribution function $f(x,V,t)$:

$$n = \int_{-\infty}^{\infty} f(V)dV,\ J_i = e\int_{-\infty}^{\infty} Vf(V)dV. \tag{2.10}$$

The boundary conditions imposed at the anode surface, $x = 0$, are

$$n_a(0,t) = n_{a0},\quad \partial T/\partial x = 0,\quad f(0,V,t) = f_0(V), \tag{2.11}$$

where $f_0(V) = \frac{\pi}{2}\frac{n_0}{V_0^2}V\exp[-\frac{\pi}{4}\frac{V^2}{V_0^2}]$ $(V > 0)$ [10, 12]. At the channel exit, $x = L$, we set

$$T = T_0. \tag{2.12}$$

The magnetic field and the plasma conduction are defined in the same way as in the fluid model. However, the ionization rate is now expressed as a function of the electron temperature: $\beta = \beta_0(T/\tilde{T} - 1)$ when $T \geq \tilde{T}$, and $\beta = 0$ otherwise [10]. The electron heat conduction coefficient is approximated as $\kappa_e = \kappa_0 T/B$, the electron temperature at the channel exit $T_0 = 20$ eV, the ion production cost $\alpha = 40$ eV, $\beta_0 = 2.2 \times 10^{-14}$ m^3/s, and $\tilde{T} = 4$ eV [10, 12].

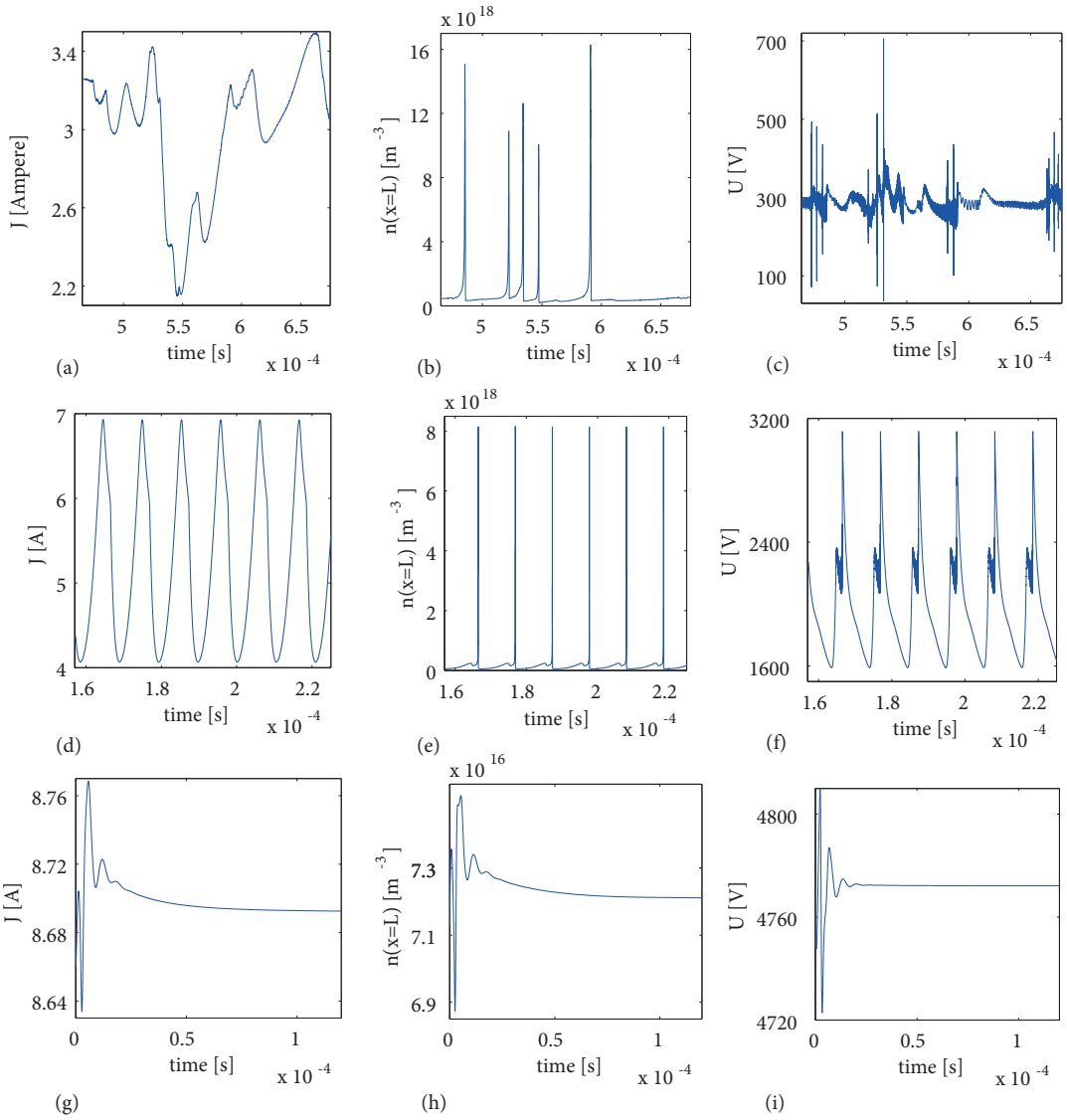

Figure 2. Time evolutions of $J(t)$, $n(x=L,t)$, and $U(t)$ in the irregular aperiodic regime (upper panel, $U_0 = 300$ V), periodic regime (middle panel, $U_0 = 2000$ V), and stable regime (lower panel, $U_0 = 4800$ V), obtained from the fluid model. Flow rate is $\dot{m} = 3.25$ mg/s.

3. Results and discussion

We consider a practically important range of Hall-effect thruster parameters, such that the inputs to the numerical code are the xenon flow rate, $\dot{m}$, within the range $2.5-5$ mgs^{-1}, and the discharge voltage, U_0, within the range $300-500$ V. The channel length is $L = 3$ cm. The ionization rate is taken as $\beta = 5 \times 10^{-14}$ m^3/s, which is the ionization rate of Xe at $T_e = 15$ eV. The neutral atom velocity at the anode is $V_a = 200$ m/s. Then, for a channel cross-sectional area of $A = 25$ cm^2, the neutral atom number density is calculated from $n_{a0} = \dot{m}/MAV_a$ as $n_{a0} = 3 \times 10^{19}$ m^{-3} [9]. The value of the channel resistivity is estimated as $R = 0.008$ m^2, such that it leads to a stationary solution with a total discharge current of $J = 3$ A under $U_0 = 300$ V and thus ensures a good agreement with the experiment [10, 12].

In order to simplify the analysis, both the fluid and hybrid models were nondimensionalized by rescaling all parameters and fields in Eqs. (2.1)–(2.6) and (2.7)–(2.12) so that the dimensionless forms of these models were subjected to numerical analysis.

3.1. Fluid model: stationary solutions

First we studied the stationary operating regime. The stationary solutions were obtained from the system of ordinary differential equations (ODEs), which were derived from Eqs. (2.1)–(2.3) and (2.5) by canceling time derivatives. The solution procedure was iterative. Starting from some estimation for current J, spatial profiles of plasma parameters and electric field were found from solution of the system of ODEs describing the stationary model. Then, using this solution, the value of the current J was updated from the circuit equation. This procedure was repeated until a convergent solution was obtained. We applied the Runge–Kutta method for ODEs on a uniform computational grid.

Figure 1 shows the axial profiles of the main thruster parameters. These profiles are obtained for different discharge voltages, $U_0 = 300 - 500$ V, while the propellant flow rate is held constant, $\dot{m} = 3.25$ mg/s. At $x/L \approx 0.2$, the ion number density reaches its maximum, which is $(7.5 - 9)\, n_0$ for the given range of input discharge voltages. At $x/L = 0.25$, neutral atoms are depleted and the propellant gas is almost fully ionized. Then the flow accelerates to a velocity of about $(10 - 12)\, V_0$ at the channel exit. The electric field and the ion velocity profiles shift upwards with the increasing discharge voltage. The neutral atom density profile remains almost the same at different discharge voltages. The profiles plotted in Figure 1 agree well with results in [10, 11], where velocity at exit is $10\, V_0$ and maximum of the ion density is $8\, n_0$ for $U_0 = 400$ V and $\dot{m} = 3$ mg/s.

As almost all the neutral atoms become ionized towards the channel exit, only ions contribute to the thrust, which can be expressed as

$$T = \dot{m} V_{\mathrm{ex}}. \tag{3.1}$$

The efficiency η of the thruster is defined as the ratio of jet power to the input power, $\eta = P_{\mathrm{jet}}/P_{\mathrm{in}}$ [3]. The jet power is $P_{\mathrm{jet}} = T^2/2\dot{m}$. Since most of the power goes into the discharge, the discharge power $P_{\mathrm{d}} = JU_0$ must be approximately equal to the input power [4], so that the efficiency becomes

$$\eta = \frac{T^2}{2\dot{m} J U_0}. \tag{3.2}$$

Calculations showed that for the discharge voltages U_0 from 300 to 500 V the discharge current J varies almost linearly from 3.00 to 3.25 A; the thrust increases from 66 to 87 mN with voltage from this range, but this cannot compensate the high discharge power input, which results in a decrease in thruster efficiency from 0.745 to 0.695.

3.2. Fluid model: transient solution and oscillation regimes

The stability of the steady solutions is studied by employing them as initial conditions for the time-dependent equations. Time evolutions of plasma parameters are calculated by using the first-order upwind scheme on the same uniform grid used in the stationary solution. Time step Δt is determined according to the Courant–Friedrichs–Lewy (CFL) condition ($\Delta t = C\, \Delta x/\max(V)$ where $C < 1$) and updated at each time iteration as $\max(V)$ changes with time.

The steady solution for $U_0 = 300\ V$ is found to be unstable. Moreover, oscillations of the discharge current $J(t)$ (Figure 2a), the ion number density $n(x = L)$ at the channel exit (Figure 2b), and the channel voltage $U(t)$ $(= \int Edx)$ (Figure 2c) are aperiodic as seen in the upper panels of Figure 2.

In [10, 11], the behavior of the transient solution in the fluid model was studied dependent on the dimensionless parameter χ, which controlled the magnitude of the ion current through the discharge channel. (Solutions demonstrated in the upper panels of Figure 2 correspond to $\chi = 255$.) It was observed that for sufficiently small values of χ stationary solutions were stable. With increase in χ periodic solutions emerged. If χ was increased further, the solution described unsteady aperiodic oscillations of the plasma parameters. In fact, in the latter case the discharge voltages fell into the range of practical interest, $U_0 = 200 - 600$ V.

In the present study, in order to reveal the effect of the parameter χ as mentioned in [10, 11], the discharge voltage was increased to sufficiently large values even though these voltages are not realistic for the operation conditions of Hall thrusters. Middle and lower panels of Figure 2 present the evolutionary behavior of $J(t)$, $n(x = L, t)$, and $U(t)$ for χ values of 38 and 16, which correspond to discharge voltages of 2000 and 4800 V, respectively, in the case of channel resistivity $R \approx 0.008\ \ \Omega m^2$. Oscillations are periodic in the first case and damped in the second, confirming the prediction in [11] that solutions become stable with sufficiently small χ.

Destabilization of the stable stationary state that evolves into a periodic oscillatory state, as parameter χ goes through certain critical values, in dynamical terms, is classified as Hopf bifurcation. Solution profiles illustrating this transition correspond to the 3rd (panels g, h, i) and 2nd (panels d, e, f) rows in Figure 2. The regime depicted in the 1st row (panels a, b, c) in Figure 2, which appears to be highly sensitive to small changes in initial conditions, is evidently in fully chaotic state. It is interesting to note that the typical route to temporal chaos that has been observed in many gas discharge systems (see, e.g., [13–16]) consists of a period doubling bifurcation cascade. Therefore, it is reasonable to expect existence of oscillatory states corresponding to the discharge voltage U_0 between 2000 and 4800 V, oscillating with periods equal to even integer multiples of that at $U_0 = 2000$ V.

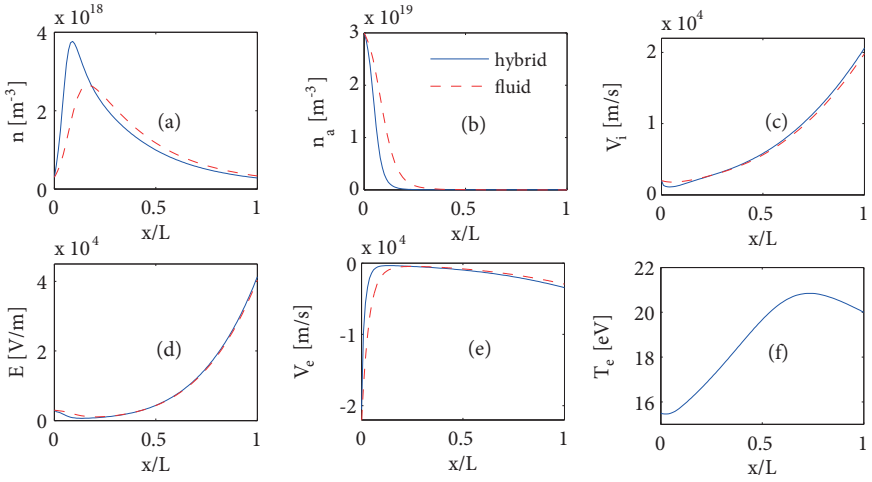

Figure 3. Spatial profiles of the plasma parameters in the discharge channel obtained from stationary fluid and hybrid models: (a) ion number density, (b) atom number density, (c) ion velocity, (d) electric field, (e) electron velocity, (f) electron temperature. Discharge voltage U_0 =300 V, flow rate $\dot{m} = 3.25$ mg/s.

3.3. Hybrid model: stationary solutions

In the hybrid modeling, the time-independent form of the Vlasov equation (Eq. (2.7)) is solved using the first-order upwind method, proceeding step by step along the discharge channel axis in the direction from the channel base to its exit. The computational grid is now two-dimensional. Since the electric field grows sharply towards the channel exit, the uniform grid previously used in the x-direction does not yield a sufficiently accurate solution. Instead, a nonuniform grid is used with decreasing step sizes towards the channel exit determined according to the CFL condition, which in dimensional form becomes $\Delta x = C(M/e)\Delta V/\max(E/V)$ with $C < 1$. As in the fluid model, stationary current value J is found iteratively, using a relaxation in order to increase stability of the iteration procedure.

Figure 3 shows the axial profiles of the main plasma parameters in the discharge channel of the thruster. When the results of the fluid and the hybrid models are compared, it is seen that the electric field and mean ion velocity profiles are nearly the same. The ion mean velocity reaches $\approx 10V_0$ at the channel exit. On the other hand, the ionization takes place closer to the anode in the hybrid model. The atoms are depleted before $x/L \approx 0.2$. The electron temperature varies only slightly. The temperatures near the anode surface are found higher than expected. As a consequence, near the channel base the ionization rate parameter is higher in the hybrid model than in the fluid model. Therefore, the ionization region shifts slightly to the left. The electron velocity increases near the anode and reaches $\approx 10V_0$.

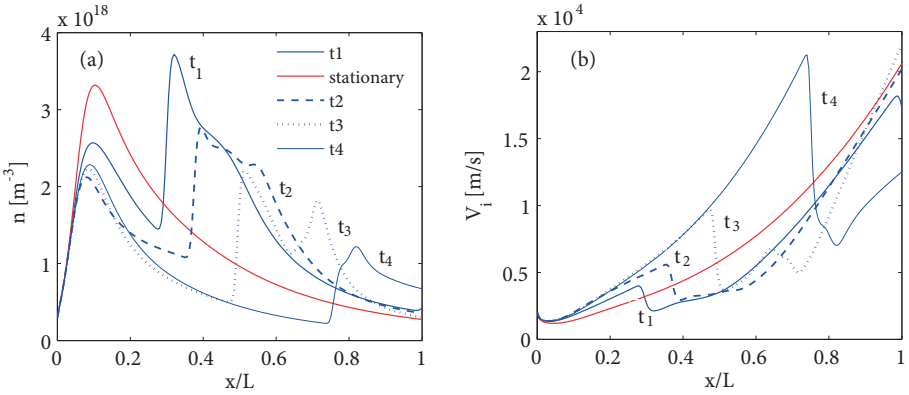

Figure 4. Hybrid model. Spatial profiles of (a) ion number density and (b) ion velocity at different instants of time. $t_1 = 0.45$ ms, time step is 2.5 μs, $\dot{m} = 3.25$ mg/s, and $U_0 = 300$ V.

3.4. Hybrid model: transient solutions

Figure 4 shows the evolution of the axial profiles of the ion number density and the ion velocity with time. Contrary to the stationary solutions, the profile of the transient solution is not monotonic but has some peaks and troughs. As can be seen, peaks and troughs of the ion number density profile correspond to troughs and peaks of the ion mean velocity profile. The peaks appear at the right side of the ionization region. At the instant as the peak's amplitude reaches the maximum, the profile begins to propagate along the channel to the right (to the channel exit), conserving its shape while its amplitude decreases. As an ion density peak approaches the channel exit, a new one appears at the ionization region and the same process repeats over and over again.

Figure 5 demonstrates the time-dependent behavior of the discharge current $J(t)$, the channel voltage $U(t)$, and the ion number density at the channel exit $n(x = L)$, for the input parameters $\dot{m} = 3.25$ mg/s

and $U_0 = 300$ V. Despite the irregular oscillations of these variables for the same input parameters in the fluid model, the hybrid model yields periodic oscillations with the main period $\tau = 50$ μs. This is due to the fact that transitions from stable to periodic and from periodic to aperiodic regimes occur at lower discharge voltages in the hybrid model than in the fluid model. Therefore, while a discharge voltage value of practical interest commonly used on thrusters such as 300 V falls into the chaotic regime in the fluid model, it remains within the periodic regime in the hybrid model. Thus, the hybrid model turns out to be more stable than the fluid model. The oscillation frequency calculated as 20 kHz for $U_0 = 300$ V agrees with the results in [9] where frequencies are found as $15 - 22$ kHz for the voltage range $200 - 350$ V.

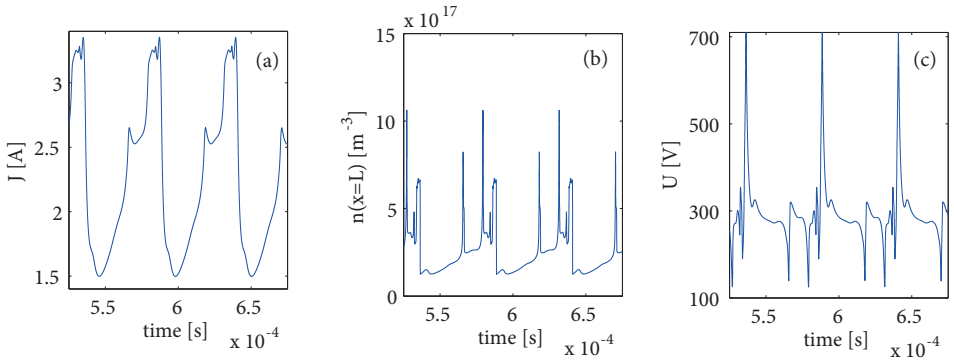

Figure 5. Hybrid model. Time evolutions of (a) $J(t)$, (b) $n(x = L, t)$, (c) $U(t)$ for $\dot{m} = 3.25$ mg/s and $U_0 = 300$ V.

4. Conclusion

One-dimensional fluid and hybrid fluid–kinetic numerical codes for a Hall-effect thruster were developed and applied to the analysis of distributions of plasma properties in the acceleration channel of the thruster.

Stationary and evolutionary regimes were investigated. Thrust and efficiency of the thruster for different input parameters were estimated.

First, stationary solutions for the plasma parameters in the discharge channel of the thruster were obtained. Then time-dependent evolution of these parameters were studied as perturbations from the corresponding steady states.

The results of the fluid and hybrid models were compared. The stationary profiles corresponding to these models were found to be close to one another.

Within the time-dependent solution, different operating regimes (damped, periodic, and aperiodic irregular oscillations about the stationary state) are revealed depending on the discharge voltage. The hybrid model turns out to be more stable than the fluid model.

Although the models are based on many approximations, they reproduce qualitatively the basic features of the thruster. The results corresponding to the stationary regimes are in good agreement with the reference models [2, 9–12]. A quantitative discrepancy that can be observed in unsteady solutions may be explained by differences in the parameter regimes studied and the initial conditions. It should also be noted that particularly in the case of the aperiodic irregular (chaotic) oscillatory regime, the solution becomes highly sensitive to small changes in initial conditions. In this case, given the model, under exactly the same conditions, even differences in numerical implementation will lead to completely different solutions. The overall accuracy of the model can be improved, for instance, by formulating the problem in two space dimensions and by taking the plasma wall interactions into account.

References

[1] Randolph, T. M. In *30th International Propulsion Conference*, Florence, Italy, 17–20 September 2007; IEPC Paper 2007-271.

[2] Morozov, A. I. *Introduction to plasma dynamics*; CRC Press: Boca Raton, FL, USA, 2012.

[3] Goebel, D. M.; Katz, I. *Fundamentals of Electric Propulsion: Ion and Hall Thrusters*; John Wiley & Sons: New York, NY, USA, 2008.

[4] Kwon, K.; Walker, M. L.; Mavris, D. N. *Plasma Sources Sci. T.* **2011**, *20*, 045021.

[5] Ahedo, E.; Martinez-Cerezo, P.; Martinez-Sánchez, M. *Phys. Plasmas* **2001**, *8*, 3058-3068.

[6] Szabo, J. Jr. PhD, Massachusetts Institute of Technology, Cambridge, MA, USA, 2001.

[7] Lentz, C.; Martinez-Sanchez, M. In *29th Joint Propulsion Conference and Exhibit*, Monterey, CA, USA, 28–30 June 1993; AIAA Paper 93-2491.

[8] Fife, J. M. PhD, Massachusetts Institute of Technology, Cambridge, MA, USA, 1998.

[9] Boeuf, J.; Garrigues, L. *J. Appl. Phys.* **1998**, *84*, 3541-3554.

[10] Morozov, A.; Savelyev, V. In *Reviews of Plasma Physics*; Kadomtsev, B. B.; Shafranov, V. D., Eds. Springer: Boston, MA, USA, 2000, pp. 203-391.

[11] Morozov, A.; Savel'ev, V. *Plasma Phys. Rep.* **2000**, *26*, 219-224.

[12] Morozov, A.; Savel'ev, A. *Plasma Phys. Rep.* **2000**, *26*, 875-880.

[13] Klinger, T.; Schröoder, C.; Block, D.; Greiner, F.; Piel, A.; Bonhomme, G.; Naulin, V. *Phys. Plasmas* **2001**, *8*, 1961-1968.

[14] Braun, T.; Lisboa, J. A.; Francke, R. E.; Gallas, J. A. *Phys. Rev. Lett.* **1987**, *59*, 613-616.

[15] Pugliese, E.; Meucci, R.; Euzzor, S.; Freire, J. G.; Gallas, J. A. *Sci. Rep.-UK* **2015**, *5*, 8447.

[16] Rafatov, I. *Plasma Sources Sci. T.* **2016**, *25*, 065014.